ISBN: 978-628-96613-1-6. ISSN: 2414-6390. Digital Object Identifier: https://dx.doi.org/10.18687/LACCEI2025.1.1.1391

Numerical Study of Pressure Gradients of a Laminar Incompressible Fluid Flow with Particles Between Two Parallel Plates

Carlos J. Amaya C[1], Julio C. Marín B[2], Orlando M. Ayala H[3], Orlando F. Ayala[4]

[1, 2, 4]Universidad de Oriente, Venezuela, *amayacabrera17@gmail.com, juliocmb99@gmail.com, ofar.ayalah@gmail.com*
[3]Old Dominion University, USA, *oayala@odu.edu*

***Abstract*– Particle transport is essential in industries such as mining, oil and gas, chemicals, and food processing, often resulting in two-phase flows. This paper investigates pressure gradients in a two-dimensional, laminar, incompressible fluid with suspended particles between two parallel plates. The model is developed using COMSOL Multiphysics 6.0, employing the finite element method. A laminar water flow serves as the continuous phase, while fluid-particle interactions are modeled through bidirectional coupling in a time-dependent framework. Key parameters influencing pressure gradients include volume fraction (αp), relative particle size (RSp), Stokes number (St) and particle release position. The variations in pressure gradients are analyzed using comparative plots, contrasting the pressure gradient with particles against the fluid-only case along the plate. Three distinct zones emerge: (1) an acceleration zone, where the pressure difference increases to a peak, (2) a transition zone, where the difference declines, and (3) a stabilization zone, where the difference becomes negligible. The results highlight the impact of volumetric particle flow rate, with higher values significantly altering pressure gradients. A decrease in relative particle size leads to greater concentration of smaller, denser particles, showing an inverse proportionality effect. As the Stokes number increases, particles exhibit greater independence from the fluid, and their increased inertia slows the full development of pressure gradients. Additionally, the particle release position plays a crucial role, particularly when particles are introduced at the center of the flow. Notably, the sum of pressure differences for particle release at the center and edges equals that of a uniform release across the entire entrance. These findings offer valuable insights into fluid-particle interactions in laminar regimes, contributing to a better understanding of their behavior under varying conditions, which may have practical implications for multiple industrial applications.**

Keywords: particle-laden flows, pressure gradients, laminar regime, Stokes number, Particle volume fraction, particle relative size.

NOMENCLATURE

Re	Reynolds number
St	Stokes number
τ_p	Particle respond time
τ_f	Fluid time scale
α_p	Particle volume fraction
RS_p	Particle relative size
U	Fluid inlet velocity
ρ_p	Particle density
ρ_f	Fluid density
ν_f	Kinematic viscosity of the fluid
Le	Entrance length
$\dot{V}_p$	Particle flow rate
$\dot{V}_f$	Fluid flow rate
d_p	Particle diameter
l_p	Average distance between particles
$t_{release}$	Release time
U_p	Velocity in the x component of the particle
U_f	Velocity in the x component of the fluid
N_p	Number of particles
$\left(\frac{dP}{dx}\right)$	Pressure gradient

I. INTRODUCTION

Two-phase flows play a crucial role in various industries, including pharmaceuticals, biomedical applications, mining, petrochemicals, nuclear energy, oil and gas, and metallurgy. They are also present in natural processes such as cloud droplet formation, dust storms, and sediment transport.

Particulate-laden flows are increasingly gaining industrial interest due to their impact on operational efficiency and safety. This topic continues to be a major area of research, as it presents common challenges for both engineers and end users. To enhance the performance, reliability, and safety of fluid transport systems, further studies are needed on how suspended particles influence fluid behavior.

Flows containing particles exhibit significantly different behavior compared to single-phase flows. Key factors such as particle size, concentration, inertia, velocity, and release position must be considered, as they influence pressure gradients. This research aims to investigate fluid-particle interactions in a two-dimensional system confined between parallel plates using computational fluid dynamics (CFD) simulations.

To address this complex topic, previous studies serve as a foundation. Research by O. M. Ayala, G. Flores & J. Laurency (2024) [1]., E. González & L. Navarrete (2023) [2]., J. Marin & C. Amaya (2023) [3]., Lin, S. (2021) [4]., M. Klazly & G. Bognar [5]., D. Vasco-Calle, D. Chen, & J. Acevedo-Cabello [6]., has highlighted the significant impact of particle volume fraction, release position, inertia, and particle size on flow behavior. These studies primarily focused on flow between flat plates and within cylindrical ducts.

In this study, a two-dimensional flow within parallel plates is analyzed, with particular emphasis on the effects of key parameters on pressure gradients. Additionally, the influence of particle response time, represented by the dimensionless Stokes number, is examined.

To conduct this research, COMSOL Multiphysics v. 6.0 [7] is employed, as it provides an interface capable of modeling fluid-particle interactions in laminar flow under a time-dependent framework.

II. PHYSICAL AND NUMERICAL MODEL

The system consists of two parallel horizontal plates (Figure 1a) with a length of $L = 2.25$ m and a separation of $H = 0.01$ m. The chosen length ensures full flow development in the analyzed cases. As depicted in Figure 1c, the model incorporates the following boundary conditions: an inlet velocity condition, an outlet pressure condition, a no-slip wall condition, and a symmetry condition. Additionally, a sliding wall condition was introduced near the inlet to create a transition zone. This initial region minimizes numerical errors caused by singularities at the corners, which would otherwise be influenced by two conflicting velocity conditions (inlet velocity and zero velocity). To simplify the model, the symmetry condition was applied, allowing the study to focus on the lower half of the domain.

The continuous phase is modeled as an incompressible, isothermal, laminar flow with a Reynolds number of $Re = 500$. Water at $T = 20°C$ is used, with a constant density of 998.2 kg/m³ and a dynamic viscosity of 1.007×10^{-6} kg/m·s [8]. The dispersed phase consists of spherical solid particles introduced at the same velocity as the fluid. Particle release is randomly distributed along the inlet boundary, and the outlet is set to a gauge pressure of 0 Pa.

This study is conducted in an unsteady-state framework, modeling the phenomenon over 54 seconds to ensure that a quasi-steady state is reached. The results are averaged over approximately the last 15 seconds for analysis.

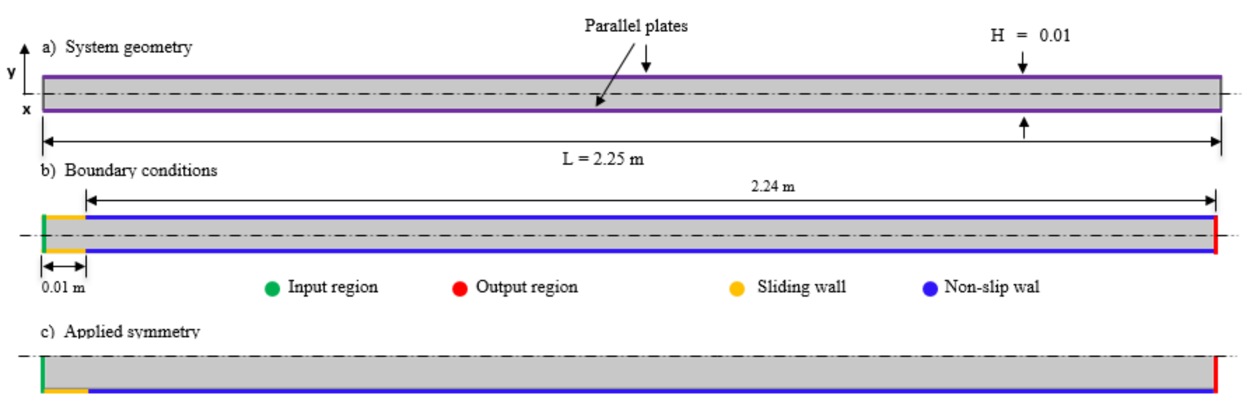

Figure 1. Physical model of parallel plates

The equations defining the flow are as follows:

Reynolds number (Re):

$$Re = \frac{U * H}{\nu_f} \quad (1)$$

where, U represents the characteristic fluid velocity, H the characteristic length, νf tdhe kinematic viscosity of the fluid.

The entrance length, which denotes the distance required for the free flow of particles to stabilize after entering the anti-skid plates, is calculated by the following equation:

$$Le = 0.04 * Re * H \quad (2)$$

where, Re represents the Reynolds number and H is the characteristic length

Regarding the parameters related to the particles, we have volume fraction (α_p), Stokes number (St) and relative particle size (RS_p), which are the key parameters of this research. The variation of these parameters is used to analyse the fluid-particle behaviour. The particle volume fraction denotes the volumetric concentration of particles in the dispersed phase relative to the total volume of the fluid:

The particle volume fraction denotes the space occupied by the dispersed phase relative to the total volume of the fluid-particle mixture [9]. It is calculated by the following equation:

$$\alpha_p = \frac{\dot{V}_p}{\dot{V}_f} \quad (3)$$

where $\dot{V}_p$ represents the volume of the dispersed phase, and $\dot{V}_f$ the volume of the total fluid with particles.

The relative particle size is a dimensionless parameter denoting the particle size (d_p) about the distance between plates (H):

$$RS_p = \frac{d_p}{H} \quad (4)$$

The Stokes number (St) is defined as the ratio between the characteristic time of a particle and the characteristic time of the flow. Particles with a low Stokes number follow the streamlines of the fluid, while for a large Stokes number, the inertia of the particle dominates so that the particle will continue its initial trajectory. It is defined by:

$$St = \frac{\tau_p}{\tau_f} \quad (5)$$

where τ_p denotes the particle response time and τ_f denotes the characteristic time of the fluid. These characteristic times follow these equations:

$$\tau_p = \frac{\rho_p * d_p^2}{18 * \rho_f * \nu_f} \quad (6)$$

$$\tau_f = \frac{L_e}{U} \quad (7)$$

where d_p represents the diameter of the particle, L_e the entrance length, and U the characteristic velocity.

We also look at the mean inter-particle distance because, to be consistent with the constant particle volume fraction throughout the simulation and the entire domain, the particle release time must be set correctly. This mean distance is the average physical separation between two particles in a flow and is calculated with the following equation [9]:

$$l_p = \left(\frac{\pi}{6 * \alpha_p}\right)^{1/3} * d_p \quad (8)$$

where α_p denotes the particle volume fraction, and d_p the diameter of the particle.

As for the particle release time at the inlet, then it is defined as follows:

$$t_{release} = \frac{l_p}{U} \quad (9)$$

where l_p represents the distance between particles and U the characteristic velocity.

With the same idea of volume fraction consistency, the number of particles entering the system per release is:

$$N_P = \frac{\alpha_p * H * d_p * l_p}{\frac{\pi}{6} * d_p^3} \quad (10)$$

where α_p is the particle volume fraction, H the characteristic length, d_p the particle diameter, and l_p the distance between particles.

A. Construction of the Mesh

A structured mesh was used for the domain. Given that the horizontal edge is 450 times longer than the vertical edge(from the wall to the line of symmetry), the mesh was designed to include 450 times more edge elements along the wall and symmetry lines (see Figure 2). The initial mesh setup included 20 edge elements (NEE) along both the leading and trailing edges, resulting in a total of 9,000 elements along the wall and symmetry edges. To enhance accuracy in critical regions affecting the pressure gradient, additional mesh refinement was applied near the leading and trailing edges, with smaller elements concentrated near the wall. An element ratio of 10 was implemented, meaning the element size near the line of symmetry is 10 times larger than that near the wall. Once the edge elements were defined, the full-domain mesh was generated and plotted for analysis.

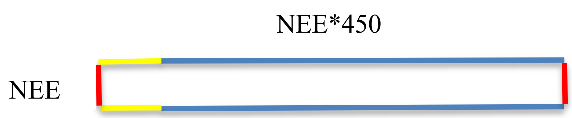

Figure 2. Diagram of the distribution of elements applied to the mesh

To assess mesh sensitivity, we evaluated the friction coefficient along the wall. The selected parameters for this analysis included a Reynolds number of 500, a volume fraction (αpαp) of 10%, a relative particle size of 0.3%, and a Stokes number of 10. The number of edge elements (NEE) was varied in increments of 20, as detailed in Table 1. The percentage difference in friction coefficients for each mesh was calculated relative to the finest mesh (Mesh 4), as illustrated in Figure 3.

TABLE I
DATA OF THE MESHES USED FOR THE SENSITIVITY ANALYSIS WITH PREDEFINED ELEMENTS

DATA OF THE MESHES		
Mesh	NEE	Size of elements (m)
1	20	$2.50\text{x}10^{-04}$
2	40	$2.30\ \text{x}10^{-04}$
3	50	$1.80\ \text{x}10^{-04}$
4	60	$1.50\ \text{x}10^{-04}$

From Figure 3, it can be concluded that Meshes 2 and 3 produce numerically identical results to Mesh 4. Therefore, Mesh 3 was selected as the final mesh for this study.

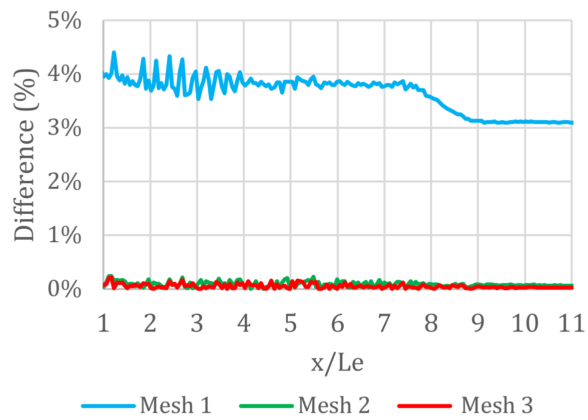

Figure 3. Refining with predefined elements: Percentage relative error of the coefficient of friction profile at the edge of the plate.

The study was conducted using the Eulerian method for the continuous phase, governed by the Navier-Stokes equations, while the Lagrangian method, governed by Newton's second law, was applied to the dispersed phase.

III. DISCUSSION AND RESULTS

This section evaluates pressure gradients in a two-dimensional, laminar, incompressible fluid with suspended particles between two parallel plates. The particle parameters were varied as follows:

- Volume fraction (αpαp): 2% to 10%
- Relative particle size (RSpRSp): 0.2% to 0.4%
- Stokes number (St): 0.1 to 20

Additionally, simulations were conducted for different particle release positions at the inlet. To assess the influence of particles on fluid behavior, we calculated the pressure gradient along the wall for each case and determined the difference between the particle-laden pressure gradient and the pressure gradient of the fluid alone.

$$\%\ \text{of difference} = \frac{\left(\frac{dP}{dx}\right)_p^* - \left(\frac{dP}{dx}\right)_f^*}{\left(\frac{dP}{dx}\right)_f^*} * 100 \qquad (11)$$

where $\left(\frac{dP}{dx}\right)_p^*$ represents the pressure gradient with particles in the x-component and $\left(\frac{dP}{dx}\right)_f^*$ the pressure gradient of the fluid without particles.

A dimensionless position defined by the following equation was used:

$$\frac{x}{L_e} \qquad (12)$$

where x (m) denotes the position of the pressure gradient on the x-axis and L_e is the inlet length of the plate.

A. Volume Fraction Effects

The pressure gradient in a laminar flow is significantly influenced by the presence of particles. As particle concentration increases, fluid-particle interactions intensify, leading to local blockages and flow disturbances. These effects result in an increase in the pressure gradient, indicating a direct correlation between particle concentration and pressure distribution.

This trend is evident in Figure 4, which presents the relative percentage difference between the flow with particles and the flow without particles. The most pronounced effects occur in the region x/Le=0.5 to 6. In this analysis, the particle volume fraction (αp) was varied, while relative particle size (RSp) and Stokes number (St) were kept constant at 0.2% and 1, respectively. Each curve represents a different volume fraction (αp=2%, 4%, 6%, 8%, 10%).

Figure 4 reveals three distinct flow regions: First, the acceleration zone (x/Le=0.8 to 1), where the flow with particles experiences an initial increase in pressure due to particle influence, and the pressure difference reaches its maximum peak within this range. Second, a transition zone (x/Le=1 to 9), where particles gradually stop transferring kinetic energy to the fluid, and the pressure decreases progressively toward equilibrium. Third, a stable zone (x/Le=9 to 11), where the flow with particles behaves similarly to the flow without particles, and the boundary layer is fully developed, and particle-fluid interactions become negligible.

The presence of one particle can accelerate or decelerate the fluid locally. When two particles are introduced, this effect is doubled, leading to a linear increase in the pressure gradient. This behavior is reflected in the curves in Figure 4, where the relative percentage difference in pressure follows a proportional trend with increasing particle concentration.

Additionally, Figure 5 confirms this linearity by normalizing the relative percentage pressure difference (dP/dx) for each curve by its corresponding volume fraction. The resulting curves exhibit a high degree of overlap, reinforcing the proportional relationship between particle concentration and pressure gradient variations.

B. Particle Relative Size Effect

The pressure gradient plots in this section follow a similar pattern to those presented earlier. However, in this case, the relative particle size (RSp) was varied while keeping the volume fraction (αp = 10%) and Stokes number (St=1) constant. Each curve represents a different relative particle size: RSp =0.4%, 0.3%, and 0.2%.

The graphs indicate that an increase in relative particle size is inversely proportional to the relative percentage differences in the pressure gradient. This occurs because, at a fixed volumetric flow rate, decreasing the particle size results in a higher number of particles in the system. This higher particle concentration has a more pronounced effect on flow behavior than the individual particle size itself. When RSp is smaller, a denser concentration of particles forms within the flow. This increased particle density delays boundary layer formation due to stronger interactions between the continuous and dispersed phases. Conversely, when RSp is larger, particles become more dispersed, allowing the fluid to move more freely, which results in a faster boundary layer development.

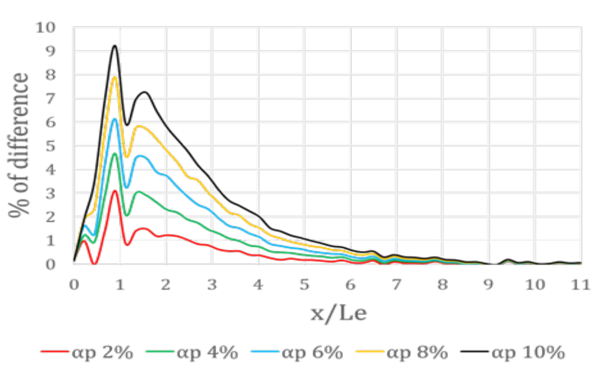

Figure 4. % difference in the pressure gradient "$\left(\frac{dP}{dx}\right)$" vs x/Le. RSp = 0.2% and St = 1.

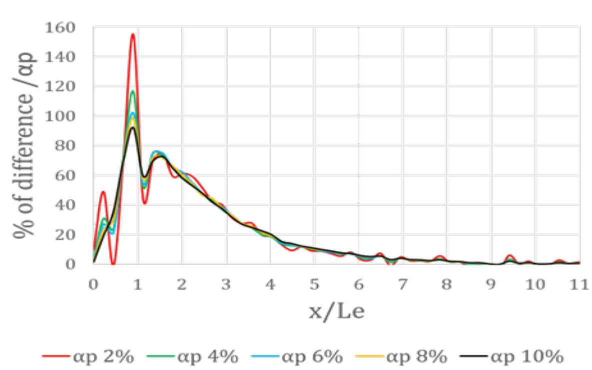

Figure 5. Percentage difference profile of the pressure gradient "$\left(\frac{dP}{dx}\right)$" vs x/Le after considering proportionality. RSp =0.2%, St=1.

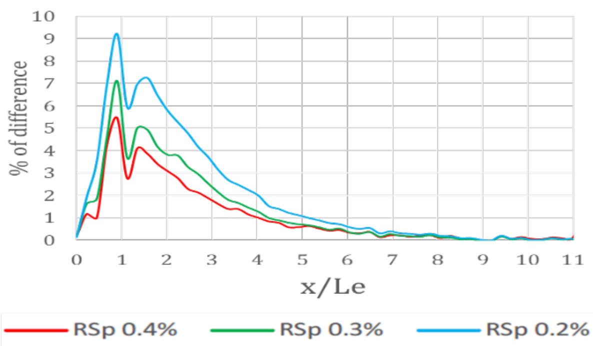

Figure 6. % difference in the pressure gradient "$\left(\frac{dP}{dx}\right)$" vs x/Le. αp = 10% and St = 1.

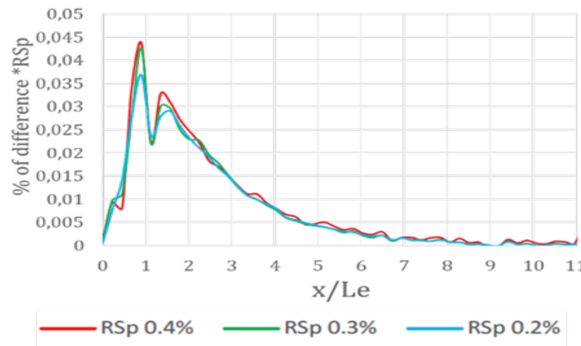

Figure 7. Percentage difference profile of the pressure gradient "$\left(\frac{dP}{dx}\right)$" vs x/Le after considering proportionality. αp = 10% and St = 1.

The impact of relative particle size on the pressure gradient is clearly illustrated in Figure 6, while Figure 7 further confirms the linear relationship between these variables.

C. Particle Stokes Number Effect

The figures in this section illustrate the relative percentage difference in pressure gradients along the x/Le position and the local Stokes number (Stx), for a volume fraction (αp = 10%) and relative particle size (RSp=0.2%).

By analyzing the variation in Stokes numbers (St), it is confirmed that as St increases, the pressure gradient difference also increases. For Stokes numbers less than 1, particles tend to follow the flow lines, since the fluid response time is longer than the particle response time, resulting in small differences that stabilize quickly. Conversely, for Stokes numbers greater than 1, particles exhibit greater inertia, increasing their independence from the fluid flow. This leads to stronger interactions, a greater pressure gradient difference, and a longer stabilization time.

For St = 5, 10, and 20, the curves indicate that flow stabilization was not achieved within the selected plate length. This suggests that a longer domain would be required to fully capture the stabilization process.

Figure 8 highlights key trends in different flow regions. In the acceleration zone (x/Le=0x/Le=0 to 1), the Stokes number has minimal influence in this region, showing a semi-proportional trend. In the transition zone (x/Le=1 to 9), the largest pressure gradient differences occur here due to particle inertia. Particles take individual paths, leading to a greater loss of kinetic energy to the fluid. And in the stabilization zone (x/Le=9 to 11), for St = 0.1 and 1, particles adapt to the continuous medium, leading to no significant difference between the dispersed and continuous phases.

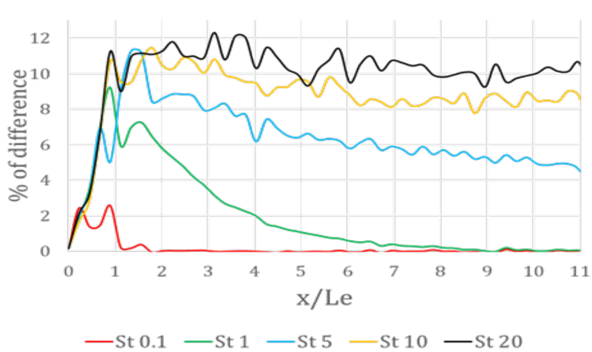

Figure 8. % difference in the pressure gradient "$\left(\frac{dP}{dx}\right)$" vs x/Le. αp = 10% and RSp = 0.2%.

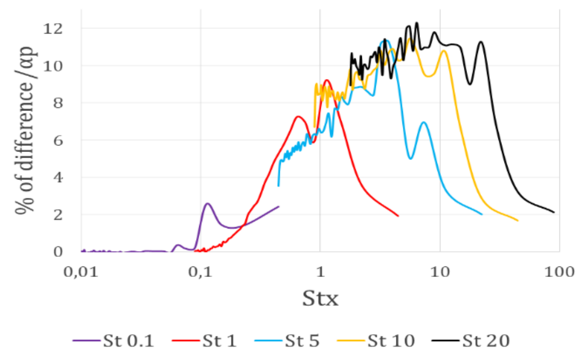

Figure 9. Percentage difference profile of the pressure gradient "$\left(\frac{dP}{dx}\right)$" vs x/Le after considering proportionality. αp = 10% and RSp = 0.2%

Figure 9 shows that Stx values consistently decrease from inlet to outlet, as Stx is position-dependent and analyzed from right to left. In the acceleration zone, Stx depends on the Stokes number, showing no proportionality. In the transition zone, however, there is no dependence on the Stokes number, meaning that variations are influenced by how the data is plotted (in relation to Stx or x/Le) rather than by St itself.

D. Effect of Particle Release Position

This section examines how particle release position affects boundary layer development. Three release positions within the same inlet region were evaluated:

1) Distributed across the entire inlet region
2) Released at the center
3) Released at the edge (near the plates)

The parameters used were αp=8%, St=1, and RSp=0.2%.

The largest relative percentage differences in pressure gradient occur when particles are distributed across the inlet region. In this case, the fluid must transfer more kinetic energy to the dispersed phase, intensifying interactions between the continuous and dispersed phases.

Figure 10 shows that centrally released particles lead to a higher-pressure gradient, whereas release at the edge has minimal effect. As the release position shifts toward the centerline between the plates, the pressure gradient increases significantly, leading to stronger fluid-particle interactions and greater flow perturbations. The highest-pressure differences are concentrated at the centerline of the plates.

This behavior aligns with the findings in Figure 11, which illustrates that the sum of relative percentage differences across the dimensionless position follows the relationship: center release + edge release = distributed.

Since edge release produces minimal differences, the distributed release and center release cases result in similar relative percentage differences.

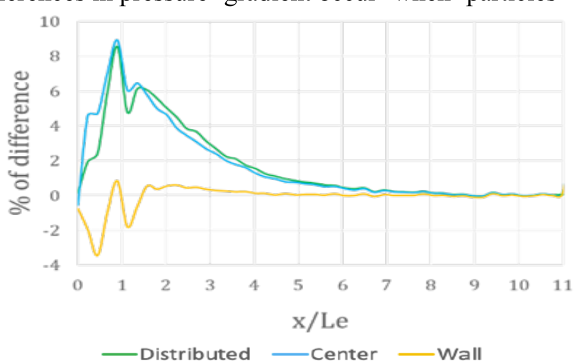

Figure 10. % difference in the pressure gradient "$\left(\frac{dP}{dx}\right)$" vs x/Le (case of particle release position). α_p=10% and RSp=0.2%.

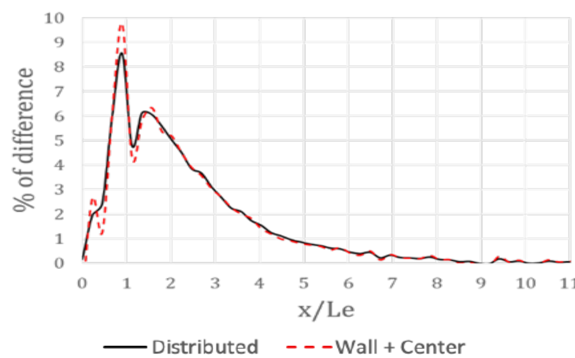

Figure 11. % difference in the pressure gradient "$\left(\frac{dP}{dx}\right)$" vs x/Le (case of particle release position

IV. CONCLUSIONS

- The pressure gradient percentage difference vs. x/Le graphs reveal three distinct flow development zones:
  1) Increase Zone – characterized by a rising pressure gradient.
  2) Transition Zone – where the pressure gradient gradually decreases.
  3) Stable Zone – where particles match the fluid velocity, and the boundary layer is fully developed.

- The extent of these zones (increase, transition, and stable) remains constant with variations in particle volume fraction and relative particle size. However, Stokes number significantly affects these zones due to changes in particle inertia.

- Increasing the relative particle size (RSp) leads to a proportional decrease in the percentage difference of the pressure gradient. When relative particle size decreases, the number of particles required to maintain the same volumetric flow rate increases. Thus, the number of particles, rather than their size, has the greatest impact on the percentage difference.

- As Stokes number increases, particles exhibit greater independence from the fluid, resulting in a longer transition period before reaching stabilization. This also affects the boundary layer development.

- Particle release position influences the pressure gradient. The increase in pressure gradient is greatest when particles are released near the plate. Additionally, the sum of the percentage differences from the central and near-wall release cases closely approximates the percentage difference in the distributed release case.

For future investigations, it is recommended to analyze particle-laden flows with smaller relative particle sizes and a longer plate length to better capture the stabilization process in cases with Stokes numbers greater than one.

REFERENCES

[1] O. M. Ayala, G. Flores, J. Laurency, "Evaluation of the fluid-particle interaction effect on the axial and radial velocity profiles of a laminar boundary layer in a pipe," *Proc. of the ASTFE 2024. American Society of Thermal and Fluids Engineers,* Corvallis, OR, USA, 2024, TFEC-2024-50097, pp. 1515-1525.

[2] E. J. Gonzalez, L. E. Navarrete, O. M. Ayala, O. F. Ayala, M. Ayala, "Numerical Study of the Friction Coefficient of an Incompressible Laminar Flow with Solid Particles Over a Flat Plate" *Proc. of the ASME 2023. International Mechanical Engineering Congress and Exposition*, New Orleans, Louisiana, USA, 2023 IMECE2023-111962, V009T10A048.

[3] J. C. Marín, C. J. Amaya, O. M. Ayala, O. F. Ayala, M. Ayala, "Numerical Study of the Velocity Profiles in an Incompressible Laminar Flow with Particles Between Two Parallel Plates" *Proc. of the ASME 2023. International Mechanical Engineering Congress and Exposition,* New Orleans, Louisiana, USA, 2023, IMECE2023-113888, V009T10A051.

[4] S. Lin, H. Xia, Z. Zhang, J. Liu, H. Wang, "Direct Numerical Simulation of Particle-laden Flow Around an Obstacle at Different Reynolds Numbers". *Journal of Physics: Conference Series*. Conf, vol 1877, Feb 2021.

[5] M. Klazly & G. Bognar, "CFD Study for the Flow Behavior of Nanofluid Flow over Flat Plate". International Journal of Mechanics. Vol. 14. Apr 2020.

[6] D. Vasco-Calle, D. Chen, & J. Acevedo-Cabello, "Computational Simulation of Laminar Heat Convection of Nanofluids in a Circular Tube and Squared Duct", DYNA, vol. 83, pp. 113-118. (2015).

[7] Comsol Inc. "COMSOL Multiphysics user's guide". (2022).

[8] V. Streeter. & B. Wiley, "Mecánica de los Fluidos". Octava Edición. Editorial McGraw-Hill Book Company. Nueva York. (1998).

[9] C. Crowe, J. Schwarzkopf, M. Sommerfeld & Tsuji, Yutaka. "Multiphase Flows with Droplets and Particles". Second Edition. Taylor and Francis Group. Florida. (2012).